Acta Crystallographica Section F
Structural Biology and Crystallization Communications
ISSN 1744-3091

Structure of a bacterial cytoplasmic cyclophilin A in complex with a tetrapeptide

Elias Christoforides,[a] Maria Dimou,[b] Panagiotis Katinakis,[b] Kostas Bethanis[a] and Michael Karpusas[a]*

[a]Physics Laboratory, Department of Science, Agricultural University of Athens, Iera Odos 75, 11855 Athens, Greece, and [b]Laboratory of General and Agricultural Microbiology, Department of Biotechnology, Agricultural University of Athens, Iera Odos 75, 11855 Athens, Greece

Correspondence e-mail: mkarp@aua.gr

Received 30 November 2011
Accepted 3 January 2012

PDB Reference: cyclophilin A–tetrapeptide complex, 3t1u.

Cyclophilins constitute a class of peptidyl-prolyl isomerases which participate in processes related to protein folding, signalling and chaperoning. The crystal structure of the cytoplasmic cyclophilin A (CyPA) from the bacterium *Azotobacter vinelandii* complexed with a synthetic tetrapeptide was determined by molecular replacement at 2 Å resolution. The proline in the tetrapeptide is observed to adopt the *cis*-isomer conformation. Comparisons of this structure with other CyPA structures provide insights into the conformational variability, effects of peptide binding and structure–function relationships of this enzyme.

1. Introduction

Cyclophilins belong to a class of peptidyl-prolyl isomerase enzymes (PPIases) which catalyze the *cis–trans* isomerization of peptide bonds preceding proline residues in protein substrates (Fischer *et al.*, 1989; Wang & Heitman, 2005). In addition to this isomerization, which accelerates protein folding, cyclophilins are involved in intracellular protein transport, chaperone activity, signal transduction, trafficking, assembly and cell-cycle regulation (Göthel & Marahiel, 1999). Cyclophilins are of significant biomedical interest because the binding of cyclophilin to cyclosporin A (CsA) mediates immunosuppressive effects that are medically utilized in the prevention of transplant rejection (Liu *et al.*, 1991). Another important activity is the binding of cyclophilin to the HIV-1 CA protein that facilitates viral replication (Luban *et al.*, 1993; Franke *et al.*, 1994; Thali *et al.*, 1994).

The determination of cyclophilin structures from a broad range of organisms has shown that the protein adopts an eight-stranded antiparallel β-barrel structure containing a peptide-binding site surrounded by mobile loops (Zhao & Ke, 1996*a*,*b*; Eisenmesser *et al.*, 2005). Structures of cyclophilins bound to propyl-peptides in the *cis* or *trans* form have provided snapshots of the enzymatic mechanism (Kallen *et al.*, 1998; Ke, 1992; Howard *et al.*, 2003). Cyclophilin has been established as a model system in enzymology in terms of extensive efforts to understand the mechanism of enzyme catalysis in full depth utilizing biochemical, structural and theoretical methods (Agarwal, 2006). Recently, there has been progress in experimental probing of the role of enzyme long-range structural dynamics in the cyclophilin enzymatic reaction (Eisenmesser *et al.*, 2005; Fraser *et al.*, 2009).

The bacterium *Azotobacter vinelandii* is a well known aerobic soil-dwelling organism relevant to agriculture which fixes atmospheric nitrogen by converting it to ammonia. The complete genome sequence of *A. vinelandii* DJ has been determined (Setubal *et al.*, 2009). There are two known cyclophilins in *A. vinelandii*: the cytoplasmic form AvPPIB (also known as AvCyPA) and the periplasmic form AvPPIA (also known as AvCyPB). Recently, we have shown that the cytoplasmic cyclophilin, but not the periplasmic cyclophilin, displays a chaperone function in the citrate synthase thermal aggregation assay (Dimou *et al.*, 2011). Furthermore, PPIase activity assays performed using succinyl-Ala-Xaa-Pro-Phe-*p*-nitroanilide tetrapeptides (where Xaa is Ala, Phe or Leu) as substrates showed that

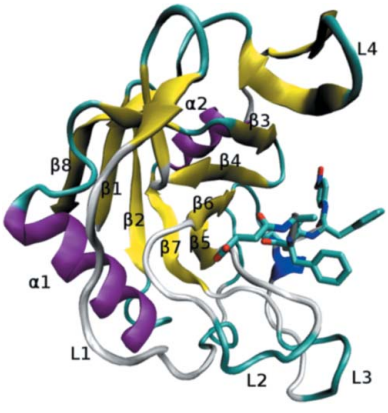

succinyl-Ala-Ala-Pro-Phe-*p*-nitroanilide is the most rapidly catalyzed substrate. Here, we report the crystal structure of cytoplasmic cyclophilin A (CyPA) from *A. vinelandii* in complex with the tetrapeptide succinyl-Ala-Phe-Pro-Phe-*p*-nitroanilide (suc-AFPF-pNA). These structural studies of CyPA from a new organism complement existing studies and further extend the body of data for a biochemically important system.

2. Materials and methods

2.1. Expression and purification of recombinant AvCyPA

The coding sequence of the AvPPIB gene (YP_002799514) corresponding to the mature encoded protein was amplified from *A. vinelandii* genomic DNA by PCR methods. Primers carrying *Bam*HI and *Xho*I restriction sites for ligation to the T7-promoter vector pET28a (Novagen) were designed and used in PCR and the amplified fragment was inserted between the corresponding sites in the pET28a vector. The absence of undesired alterations was confirmed by nucleotide sequencing (GenBank accession No. YP_002799514). *Escherichia coli* BL21 (DE3) cells (Novagen) were transformed with the vector and expression of His-tagged recombinant protein was induced in cell cultures by the addition of 0.5 m*M* isopropyl *β*-D-1-thiogalactopyranoside (IPTG) when the culture density reached an A_{600} of 0.6. Cells were harvested by centrifugation and were disrupted by sonication in lysis buffer (50 m*M* NaH_2PO_4, 300 m*M* NaCl, 10 m*M* imidazole supplemented with 1 mg ml^{-1} lysozyme). Recombinant proteins were purified by Ni–NTA size-exclusion chromatography (Ni^{2+}–nitrilotriacetate, Qiagen) according to the manufacturer's instructions. Fractions containing the eluted protein were pooled, quantified using the Bradford assay (Bradford, 1976) and dialysed against 35 m*M* HEPES buffer pH 8.0, 70 m*M* NaCl for 12 h. The purified protein, which contains a histidine tag and a mutation of residue Met1 to Ser, was >95% pure based on SDS–PAGE.

2.2. Crystal structure determination of the AvCyPA–peptide complex

Crystals of the AvCyPA–peptide complex were obtained by the hanging-drop vapour-diffusion method as follows: AvCyPA protein (8 mg ml^{-1}) in 35 m*M* HEPES pH 8.0, 70 m*M* NaCl was mixed with 5 m*M* suc-AFPF-pNA tetrapeptide, 0.45 *M* LiCl in trifluoroethanol in a 1:10 molar ratio and incubated at room temperature for 15 min. Crystallization screening using the Crystallization Basic Kit for Proteins (Sigma) produced rod-shaped crystals using several different screen conditions. After optimization of the crystallization conditions, crystallization drops were prepared by mixing 5 µl protein solution, 0.8 µl 5 m*M* peptide/trifluoroethanol/0.45 *M* LiCl and 4.2 µl precipitant buffer [19%(*w*/*v*) polyethylene glycol 8000, 0.1 *M* ammonium cacodylate, 0.1 *M* ammonium acetate] and were suspended over wells containing 1 ml of the latter. The drops initially became turbid, but became clear overnight. Bipyramid-shaped crystals grew at 291 K over a two-week period.

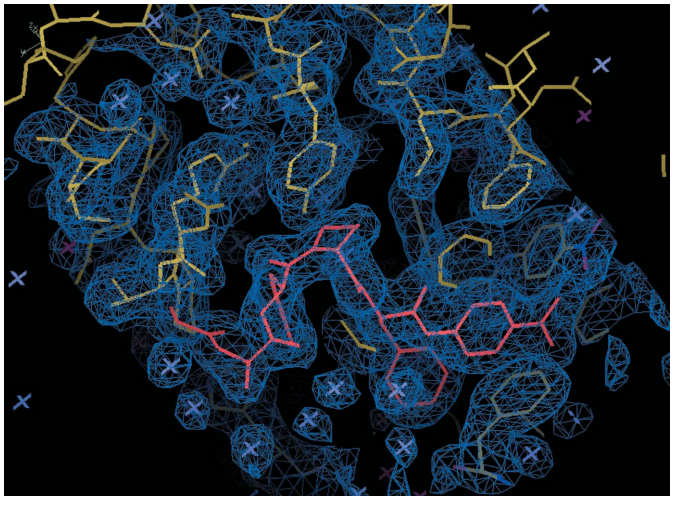

Figure 1
Representative portion of the final $2F_o - F_c$ electron-density map contoured at 1.2σ in the vicinity of the peptide-binding site. The peptide model is shown in pink. This figure was prepared with *Coot*.

Table 1
Crystallographic data-collection and refinement statistics.

Values in parentheses are for the highest resolution shell.

Space group	$P4_22_12$
Unit-cell parameters (Å)	
a	66.41
b	66.41
c	71.53
Resolution range (Å)	100.0–2.0 (2.07–2.00)
Unique reflections	11291 (1089)
Completeness (%)	99.4 (98.9)
Mean $I/\sigma(I)$	24.72 (4.76)
R_{merge}† (%)	5.4 (30.4)
R_{cryst} (%)	20.13 (23.06)
R_{free} (%)	23.81 (27.63)
Protein atoms	1245
Ligand atoms	51
Water molecules	118
Average *B* factor for protein atoms‡ (Å^2)	25.1
Average *B* factor for ligand atoms‡ (Å^2)	22.7
R.m.s.d. (bonds)§ (Å)	0.010
R.m.s.d. (angles)§ (°)	1.43

† $R_{merge} = \sum_{hkl}\sum_i |I_i(hkl) - \langle I(hkl)\rangle| / \sum_{hkl}\sum_i I_i(hkl)$. ‡ As defined by *BAVERAGE* v.6.1 from the *CCP*4 suite. § As defined by *PHENIX* (Adams *et al.*, 2010).

A crystal of approximate dimensions 0.3 × 0.3 × 0.3 mm was cryoprotected by rapid immersion in 20% PEG 400, 19%(*w*/*v*) polyethylene glycol 8000, 0.1 *M* ammonium cacodylate, 0.1 *M* ammonium acetate and flash-cooled in an N_2 stream for data collection at 100 K using a Rigaku Cu *Kα* radiation source and an R-AXIS IV image-plate detector (Rigaku MSC). Diffraction data were collected to 2 Å resolution and processed with the *HKL* program package (Otwinowski & Minor, 1997). Initial data processing indicated that the crystals were tetragonal with 422 Laue symmetry; however, the space group could not be identified at this point owing to insufficient data on systematic absences.

The structure of the AvCyPA–peptide complex was solved by molecular replacement using the program *AMoRe* (Trapani & Navaza, 2008) from the *CCP*4 program package (Winn *et al.*, 2011) with the crystal structure of cytoplasmic *E. coli* peptidyl-prolyl isomerase (Konno *et al.*, 1996; PDB entry 1lop) as the search model. Rotation and translation searches for different possible space groups resulted in a single solution corresponding to space group $P4_22_12$ with one protein molecule in the asymmetric unit. This solution had a correlation coefficient of 0.659 after initial rigid-body refinement and an *R* factor of 39.7%. The molecular model was built using the program *Coot* (Emsley & Cowtan, 2004) and was refined using *CNS* (Brünger *et al.*, 1998). 10% of the data were allocated for R_{free} calculation. Water molecules were identified with *Coot*. Cycles of model building, positional refinement and *B*-factor refinement resulted in a final model with an *R* factor of 20.13% and an R_{free} of 23.81%. Additional data-collection and refinement statistics are summarized in Table 1. Structure factors and coordinates of the

model have been deposited in the Protein Data Bank under accession code 3t1u.

3. Results and discussion

3.1. Quality of the structure

The crystal structure of cytoplasmic cyclophilin A from *A. vinelandii* (AvCyPA) was solved by molecular replacement in complex with the tetrapeptide suc-AFPF-pNA (AFPF for short). Table 1 gives the final refinement statistics and stereochemical parameters for the crystal structure. The final model for the AvCyPA–AFPF structure consists of residues 1–163 of the mature protein, the AFPF peptide and 118 water molecules. Electron density for the C-terminal residue Glu164 as well as the N-terminal His-tag residues was weak and non-interpretable; therefore, these residues were not included in the final model. The side chains of residues Lys3, Lys14, Lys32, Glu22 and Lys159 were either almost absent in electron-density maps or were associated with a much weaker density than the rest of the protein. Otherwise, the electron density was well defined (Fig. 1). The geometries of the main chain and side chains were analysed using the program *MolProbity* (Chen *et al.*, 2010). The Ramachandran plot (Ramachandran & Sasisekharan, 1968) showed that all residues (163/163) are within the allowed regions and that 94.5% (154/163) of all residues are in the favoured regions. The average *B* factors for main-chain and side-chain atoms of the protein were 24.1 and 26.2 Å^2, respectively, as defined by the program *BAVERAGE* from the *CCP*4 suite (Winn *et al.*, 2011). The average *B* factors for the main-chain and side-chain atoms of the peptide were 21.1 and 23.5 Å^2, respectively.

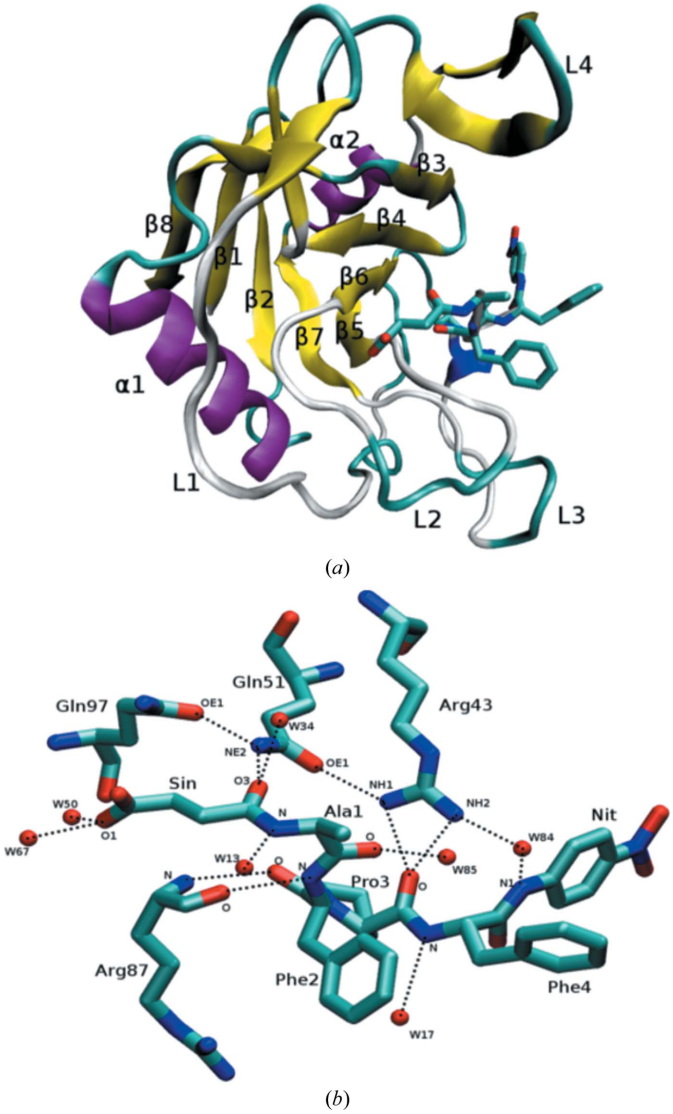

Figure 2
(*a*) Crystal structure of the AvCyPA–AFPF complex. The protein is shown as a ribbon with secondary-structure elements coloured and labelled. The dark blue colour corresponds to a 3_{10}-helix and the light blue colour to turns. The peptide is shown in stick representation. (*b*) Details of peptide binding in the vicinity of the binding site. Protein residues and water molecules involved in polar interactions with the peptide are included and hydrogen bonds are shown as dotted lines. This figure was prepared with the program *VMD* (Humphrey *et al.*, 1996).

3.2. Overall structure

CyPA from *A. vinelandii* has a similar structure to CyPAs from other organisms such as *E. coli* (Konno *et al.*, 1996) and human (Eisenmesser *et al.*, 2005). In the following description, we use names for secondary-structure elements that are consistent with the equivalent elements of *E. coli* CyPA (EcCyPA; Konno *et al.*, 1996). The structure (Fig. 2*a*) contains eight antiparallel β-strands that form two orthogonal β-sheets that are linked by hydrogen bonds to generate β-bulges. There are also two α-helices, α1 (Ala21–Asp33) and α2 (Thr130–Ile136), which close the barrel at both ends. The first β-sheet consists of strands β3 (Thr39–Ile45), β4 (Phe48–Gly53), β5 (Tyr81–Met85) and β6 (Gly97–Val102). Strands β1 (Ser1–Thr6), β2 (Gly9–Leu15), β7 (Phe123–Glu128) and β8 (Val155–Val163) form the second β-sheet. The two orthogonal β-sheets are linked to form a β-barrel. As a result of this linking, the β3 and β7 strands curl around Gly38 and His42 and around Phe123 and Val127, respectively. His42 and Val127 form β-bulges to facilitate the curling. In addition, curling occurs of strands β5 (around Tyr81) and β8 (around Glu158). The β-strands and two α-helices are connected by four long loops (L1–L4), one of which (L3) contains a short 3_{10}-helix. Finally, loop L4 contains a structure that may resemble a small β-sheet containing two small β-strands, which may enable the loop to move as a rigid body (Fig. 2*a*).

Temperature factors may give some indication of regional mobility in the structure. A plot of the average *B* factors for all atoms *versus* residue number for AvCyPA (Fig. 3) shows that loops L1, L2, L3 and

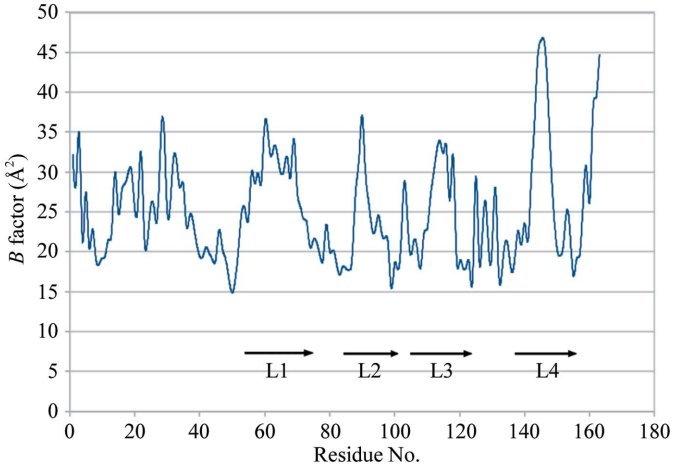

Figure 3
Plot of temperature factor *versus* residue number. Each dot corresponds to the average temperature factor for all atoms of each residue. The locations and extents of the L1–L4 loops are shown.

L4 are characterized by high mobility, as was observed in the case of EcCyPA (Edwards *et al.*, 1997).

3.3. Structure of the bound tetrapeptide

The peptide-binding site is located in a hydrophobic cleft on the surface of the molecule formed mainly by the first β-sheet (β3, β4, β5 and β6; Fig. 2), similar to previously determined CyPA–peptide structures. The hydrophobic pocket is formed by the side chains of six highly conserved hydrophobic residues (Phe48, Met49, Phe99, Phe107, Leu108 and Tyr120). The peptide proline residue (Pro3) adopts the *cis*-proline isomer and its ring is inserted into the hydrophobic pocket with an orientation parallel to the aromatic ring of Tyr120. The Pro3 residue has an envelope form in which its C^{α} atom lies above the plane of the coplanar $C^{\beta}-C^{\alpha}-N-C^{\delta}$ atoms. The φ/χ torsional angles for Ala1, Phe2, Pro3 and Phe4 in the bound tetrapeptide are $-87/-13^{\circ}$, $-98/157^{\circ}$, $-70/146^{\circ}$ and $-71/136^{\circ}$, respectively. The Phe–*cis*-Pro link of the tetrapeptide exhibits a reverse open turn, which is the minimum-energy conformation for a *cis*-proline (φ/χ range = -60° to $-120^{\circ}/120^{\circ}$ to 180°; Ramachandran & Mitra, 1976). The aromatic ring of *p*-nitroanilide at the C-terminal end of the tetrapeptide is sandwiched between the aromatic rings of Phe48 and Phe107 (from a symmetry-related molecule) and forms π–π interactions with them. The side chain of peptide residue Phe4 points towards the solvent and does not form any contacts with nearby atoms. The phenyl ring of the peptide residue Phe2 is parallel to the ring of Pro89 and appears to form stacking interactions with it.

Table 2 lists the hydrogen bonds formed between the peptide and protein. The carbonyl O atom of the peptide proline forms hydrogen bonds to both the $N^{\eta1}$ and the $N^{\eta2}$ groups of the catalytically important residue Arg43 (Arg55 in human CyPA). The Arg43 $N^{\eta1}$ group also forms a hydrogen bond to the $O^{\varepsilon1}$ atom of Gln51

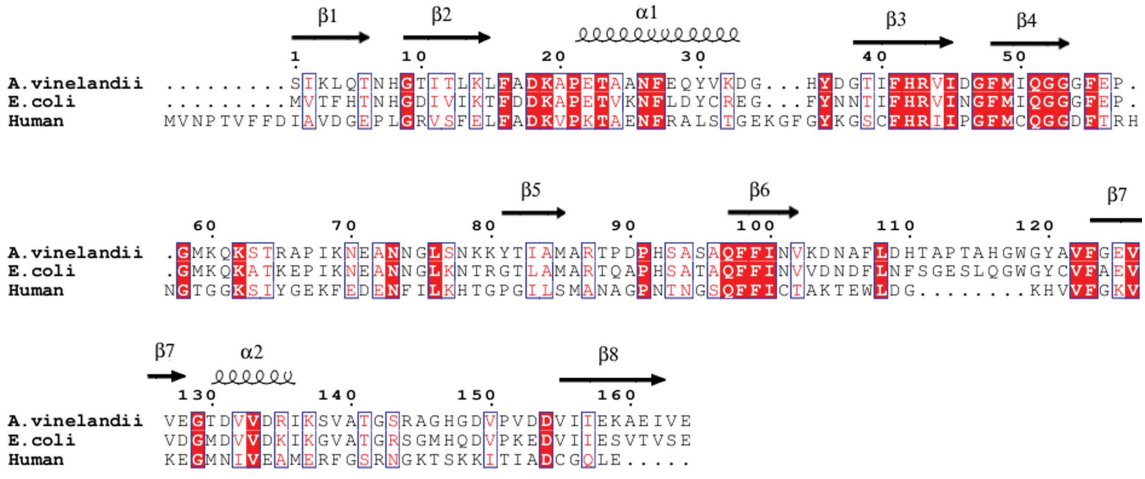

(*a*)

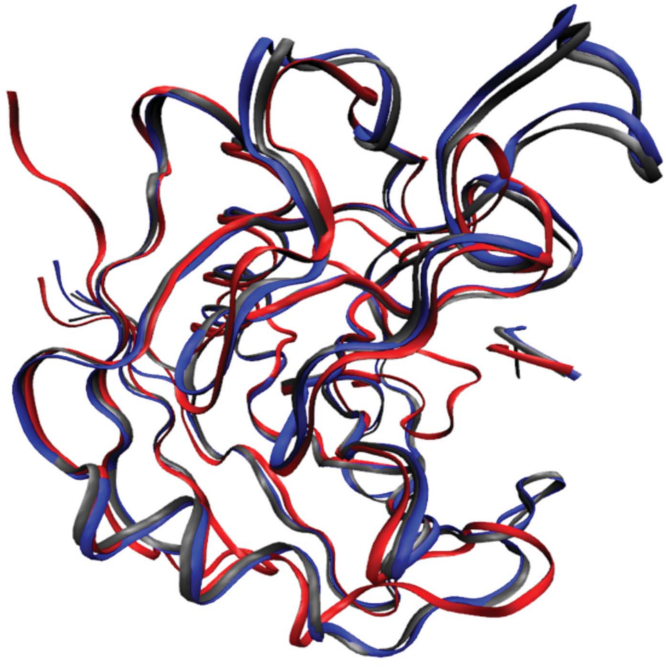

(*b*)

Figure 4
(*a*) Sequence alignment of representative CyPA molecules. Conserved residues and secondary-structure elements are shown (Gouet *et al.*, 2003). (*b*) Superimposed backbones of AvCyPA (PDB entry 3t1u; grey), EcCyPA (PDB entry 1lop, blue) and hCyPA (PDB entry 1zkf; red) crystal structures. This figure was prepared with the program *VMD* (Humphrey *et al.*, 1996).

Table 2
Hydrogen bonds and lengths (in Å).

Between the peptide and AvCyPA/water molecules		
Suc O^1	W67	2.75
Suc O^1	W50	2.56
Suc O^3	W34	2.56
Suc O^3	Gln51 $N^{\varepsilon 2}$	3.13
Ala1 N	W13	3.00
Ala1 O	W85	2.61
Phe2 N	Arg87 O	2.92
Phe2 O	Arg87 N	2.96
Pro3 O	Arg43 $N^{\eta 1}$	2.83
Pro3 O	Arg43 $N^{\eta 2}$	2.86
Phe4 N	W17	3.14
pNA N^1	W84	2.81
In the Arg43–Gln51–Gln97 network		
Arg43 $N^{\eta 1}$	Gln51 $O^{\varepsilon 1}$	2.90
Gln51 $N^{\varepsilon 2}$	Gln97 $O^{\varepsilon 1}$	2.70
Arg43 $N^{\eta 2}$	W84	3.13

(equivalent to residue Gln63 in human CyPA). Interestingly, a water molecule is also observed to form hydrogen bonds to the guanidine group of Arg43 and the N^1 atom of the peptide *p*-nitrophenyl group (which acts as a bridge between the protein and the peptide). A water molecule in the same position is also observed in human cyclophilin A complexed with succinyl-Ala-Gly-Pro-Ala-*p*-nitroanilide (PDB entry 1zkf; E. Z. Eisenmesser, V. Thai, E. Pozharski & D. Kern, unpublished work). In this structure, Arg55 and the peptide *p*-nitrophenyl group also adopt essentially identical conformations to those in AvCyPA.

The peptide residue Phe2 forms a hydrogen bond between its main-chain carbonyl and the amide of Arg87 and a hydrogen bond between its amide and the carbonyl of Arg87, resulting in a small antiparallel β-strand. The N-terminal succinyl carbonyl group forms a hydrogen bond to Gln51 $N^{\varepsilon 2}$. The succinyl carboxyl group at the peptide N-terminus also forms hydrogen bonds to two water molecules that act as bridges between the peptide and the protein.

3.4. Comparison with cyclophilin A structures from other organisms

Fig. 4(*a*) shows a sequence alignment of several representative CyPA sequences from different organisms based on least-squares structural superimposition (Larkin *et al.*, 2007; Gouet *et al.*, 2003). The sequence identity between AvCyPA and *E. coli* CyPA (EcCyPA) is 61.96% and that between AvCyPA and human CyPA (hCyPA) is 31.11%. Accordingly, the r.m.s. deviation for the positions of all superimposed C^α atoms for AvCyPA and EcCyPA (PDB entry 1lop, contains a bound tripeptide; Konno *et al.*, 1996) is 0.44 Å, while that for AvCyPA and hCyPA (PDB entry 1zkf) is 1.24 Å. Fig. 4(*b*) shows a least-squares structural superimposition of the AvCyPA, EcCyPA and hCyPA structures. The sequence and structure alignments indicate that while the hydrophobic core of the protein is conserved among a broad range of organisms, the four loop regions (L1–L4) are characterized by low residue and structure conservation as well as insertions and deletions. Thus, as expected, sequence variation appears to contribute to the variations in structure observed in cyclophilins from different sources (Edwards *et al.*, 1997).

Since AvCyPA and EcCyPA are the most closely evolutionarily related and because a comparison of EcCyPA with hCyPA has been published elsewhere (Konno *et al.*, 1996), we focus on a comparison between the AvCyPA and EcCyPA structures. The nature of the hydrophobic interactions observed in the hydrophobic core is generally conserved. For example, the hydrophobic interactions of Ile2, Leu4 and Thr6 (β1 strand) with Phe27, Phe98 and Phe41 (α1 helix, β6 and β3 strands) observed in AvCyPA are also present in EcCyPA and include some conservative substitutions such as Ile2→Val2 and Leu4→Phe4. Hydrophobic interactions also occur between Ile11, Leu13 and Leu15 (β2) with Ile100 (β6), Ile83 (β5) and Phe123 (β7) in AvCyPA (Leu13 and Leu15 are replaced by Ile13 and Thr15 in EcCyPA). At the α1 helix and T2 turn, the aromatic side chains of Phe27, Tyr30, His35 and Tyr36 make hydrophobic contacts mainly with the aromatic side chains of Phe41 (β3), Phe98 (β6) and Phe123 (β7) inside the β-barrel. On the other hand, the aliphatic side chains of Thr130, Val133 and Ile136 in the α2 helix make hydrophobic contacts with the aliphatic side chains of Ile11 (β2), Val44 (β3), Ile50 (β4), Ile83 (β5), Ile100 (β6) and Val126 (β7) inside the β-barrel.

At the periphery of the upper β-sheet in AvCyPA, the conformations of loops L1, L3 and L4 and the segment connecting α1 and β3 do not differ significantly from those in EcCyPA. Any observed differences in loops L1, L3 and L4 may arise from differences in amino-acid sequence or different crystal-packing environments. In AvCyPA, as in EcCyPA, the formation of two short β-strands consisting of five inserted residues seems to make the conformation of the L4 loop stable. Similarly, the conformation of the L1 loop is such that Phe55, Pro57 and Met59 make hydrophobic contacts with His147 of the L4 loop and Ile40 and His42 of the β3 strand in order to pack together closely.

In terms of the peptide-binding site and substrate conformation, we compared four representative structures: AvCyPA, EcCyPA (PDB entry 1lop; Konno *et al.*, 1996) and two human CyPA structures, a complex with succinyl-Ala-Ala-Pro-Phe-*p*-nitroanilide (PDB entry 1rmh; Zhao & Ke, 1996*a*) and a complex with succinyl-Ala-Gly-Pro-Ala-*p*-nitroanilide (PDB entry 1zkf; E. Z. Eisenmesser, V. Thai, E. Pozharski & D. Kern, unpublished work). The peptide backbone binds to AvCyPA in a very similar conformation to that observed for the complex of human CyPA with succinyl-Ala-Ala-Pro-Phe-*p*-nitroanilide. The side chains of Phe4 in the different peptides adopt different rotameric conformations, consistent with the fact that they are pointing out into the solvent. In general, we observe that the C-terminal portion of the peptides with *cis*-Pro binds to the enzyme in a very similar manner in all of the structures despite the π–π interaction of the *p*-nitroanilide group with a symmetry-related molecule that is observed in the case of AvCyPA. However, the N-terminal portion of the peptide adopts a considerably variable conformation in all of the structures. This variability is consistent with the evidence of Howard *et al.* (2003), in which the N-terminal portion of the peptide rotates during catalysis while the C-terminal portion remains stationary. The Arg43 side chain of AvCyPA adopts a different rotamer that does not allow the hydrogen-bond interaction of Arg43 N^{ε} with Gln51 that was observed in the EcCyPA structure (PDB entry 1lop). However, Arg43 has a very similar conformation to that observed in the complex of hCyPA with succinyl-Ala-Ala-Pro-Phe-*p*-nitroanilide (PDB entry 1rmh).

4. Conclusions

Cytoplasmic cyclophilin A from *A. vinelandii* adopts a similar structure to the closely related cytoplasmic cyclophilin A from *E. coli*. The tetrapeptide binds in a *cis*-proline isomer mode, with the C-terminal portion of the peptide adopting a commonly observed binding mode.

We thank M. Saridakis and I. Mavridis at NCSR 'Demokritos' for access and help in data collection.

References

Adams, P. D. *et al.* (2010). *Acta Cryst.* D**66**, 213–221.

Agarwal, P. K. (2006). *Microb. Cell Fact.* **5**, 2.
Bradford, M. M. (1976). *Anal. Biochem.* **72**, 248–254.
Brünger, A. T., Adams, P. D., Clore, G. M., DeLano, W. L., Gros, P., Grosse-Kunstleve, R. W., Jiang, J.-S., Kuszewski, J., Nilges, M., Pannu, N. S., Read, R. J., Rice, L. M., Simonson, T. & Warren, G. L. (1998). *Acta Cryst.* D**54**, 905–921.
Chen, V. B., Arendall, W. B., Headd, J. J., Keedy, D. A., Immormino, R. M., Kapral, G. J., Murray, L. W., Richardson, J. S. & Richardson, D. C. (2010). *Acta Cryst.* D**66**, 12–21.
Dimou, M., Venieraki, A., Liakopoulos, G., Kouri, E. D., Tampakaki, A. & Katinakis, P. (2011). *J. Mol. Microbiol. Biotechnol.* **20**, 176–190.
Edwards, K. J., Ollis, D. L. & Dixon, N. E. (1997). *J. Mol. Biol.* **271**, 258–265.
Eisenmesser, E. Z., Millet, O., Labeikovsky, W., Korzhnev, D. M., Wolf-Watz, M., Bosco, D. A., Skalicky, J. J., Kay, L. E. & Kern, D. (2005). *Nature (London)*, **438**, 117–121.
Emsley, P. & Cowtan, K. (2004). *Acta Cryst.* D**60**, 2126–2132.
Fischer, G., Wittmann-Liebold, B., Lang, K., Kiefhaber, T. & Schmid, F. X. (1989). *Nature (London)*, **337**, 476–478.
Franke, E. K., Yuan, H. E. & Luban, J. (1994). *Nature (London)*, **372**, 359–362.
Fraser, J. S., Clarkson, M. W., Degnan, S. C., Erion, R., Kern, D. & Alber, T. (2009). *Nature (London)*, **462**, 669–673.
Göthel, S. F. & Marahiel, M. A. (1999). *Cell. Mol. Life Sci.* **55**, 423–436.
Gouet, P., Robert, X. & Courcelle, E. (2003). *Nucleic Acids Res.* **31**, 3320–3323.
Howard, B. R., Vajdos, F. F., Li, S., Sundquist, W. I. & Hill, C. P. (2003). *Nature Struct. Biol.* **10**, 475–481.
Humphrey, W., Dalke, A. & Schulten, K. (1996). *J. Mol. Graph.* **14**, 33–38.
Kallen, J., Mikol, V., Taylor, P. & Walkinshaw, M. D. (1998). *J. Mol. Biol.* **283**, 435–449.
Ke, H. (1992). *J. Mol. Biol.* **228**, 539–550.
Konno, M., Ito, M., Hayano, T. & Takahashi, N. (1996). *J. Mol. Biol.* **256**, 897–908.
Larkin, M. A., Blackshields, G., Brown, N. P., Chenna, R., McGettigan, P. A., McWilliam, H., Valentin, F., Wallace, I. M., Wilm, A., Lopez, R., Thompson, J. D., Gibson, T. J. & Higgins, D. G. (2007). *Bioinformatics*, **23**, 2947–2948.
Liu, J., Farmer, J. D., Lane, W. S., Friedman, J., Weissman, I. & Schreiber, S. L. (1991). *Cell*, **66**, 807–815.
Luban, J., Bossolt, K. L., Franke, E. K., Kalpana, G. V. & Goff, S. P. (1993). *Cell*, **73**, 1067–1078.
Otwinowski, Z. & Minor, W. (1997). *Methods Enzymol.* **276**, 307–326.
Ramachandran, G. N. & Mitra, A. K. (1976). *J. Mol. Biol.* **107**, 85–92.
Ramachandran, G. N. & Sasisekharan, V. (1968). *Adv. Protein Chem.* **23**, 283–438.
Setubal, J. C. *et al.* (2009). *J. Bacteriol.* **191**, 4534–4545.
Thali, M., Bukovsky, A., Kondo, E., Rosenwirth, B., Walsh, C. T., Sodroski, J. & Göttlinger, H. G. (1994). *Nature (London)*, **372**, 363–365.
Trapani, S. & Navaza, J. (2008). *Acta Cryst.* D**64**, 11–16.
Wang, P. & Heitman, J. (2005). *Genome Biol.* **6**, 226.
Winn, M. D. *et al.* (2011). *Acta Cryst.* D**67**, 235–242.
Zhao, Y. & Ke, H. (1996*a*). *Biochemistry*, **35**, 7356–7361.
Zhao, Y. & Ke, H. (1996*b*). *Biochemistry*, **35**, 7362–7368.